

# Prediction of Temperature of Critical Viscosity for Coal Ash Slag

Wenjia Song, Yanhe Dong, Yongqiang Wu, and Zibin Zhu

The State Key Laboratory of Chemical Engineering, East China University of Science and Technology, Shanghai 200237, P.R. China

DOI 10.1002/aic.12500

Published online March 14, 2011 in Wiley Online Library (wileyonlinelibrary.com).

Keywords: coal ash slag, coal gasification, temperature of critical viscosity

## Introduction

The need for greater efficiency for future power generation has led to an increase in integrated gasification combined cycle (IGCC) technologies, which can reduce emissions of greenhouse gas, sulfur dioxide, nitrogen oxides and trace elements.<sup>1,2</sup> IGCC plants commonly utilize entrained flow gasifiers, which are generally operated in slagging mode at high-temperatures (1400–1800°C), and pressures (20–70 bar).<sup>3,4</sup> To ensure reliable slag tapping, the operation temperature of the gasifier should be above the temperature of critical viscosity of the slag,<sup>5</sup>  $T_{cv}$ . This temperature is recognized as a sharp break in the viscosity vs. temperature curve and marks the division between crystal-affected viscosity and viscosity not affected by the presence of crystals.<sup>6</sup> The difficulty and high cost of measuring the  $T_{cv}$  value of slag derived from coals with varied ash analyses has led to many predictive models based on ash fusion temperature (AFT) and chemical composition.<sup>7</sup>

## Sage Model

Sage and McIlroy<sup>8</sup> found the hemispherical temperature of coal ash slag  $T_h$ , to be an adequate guide for  $T_{cv}$

$$T_{cv} = T_h + 111 \quad (1)$$

The hemispherical temperature of coal ash is defined according to the ASTM ash fusion test as the temperature at which a cone collapses to a hemispherical lump (height =  $1/2 \times$  width).

## Corey Model

Corey<sup>9</sup> proposed a relationship between  $T_{cv}$  and the softening temperature  $T_s$ , defined as the temperature at which a cone fuses to a lump with height = width

$$T_{cv} = T_s \quad (2)$$

## Marshak Model

Marshak and Ryzhakov<sup>10</sup> also showed the  $T_{cv}$  of a coal ash slag to be a function of  $T_s$

$$T_{cv} = 0.75 \cdot T_s + 548[K] \quad (3)$$

Analysis of coal ash compositions shows that they consist mainly of  $\text{SiO}_2$ ,  $\text{Al}_2\text{O}_3$ ,  $\text{Fe}_2\text{O}_3$ ,  $\text{CaO}$ , and  $\text{MgO}$ ,<sup>11,12</sup> so that the properties of coal ashes at high-temperature might be modeled by a five component  $\text{SiO}_2$ - $\text{Al}_2\text{O}_3$ - $\text{Fe}_2\text{O}_3$ - $\text{CaO}$ - $\text{MgO}$  synthetic ash. Moreover, since the composition of synthetic ash samples can be easily controlled, the experimental conditions can be simplified and can exclude any interference by trace elements. Thus, we have measured the  $T_{cv}$  values of 40 synthetic ash samples formed by mixtures of these five oxides ( $\text{SiO}_2$ ,  $\text{Al}_2\text{O}_3$ ,  $\text{CaO}$ ,  $\text{Fe}_2\text{O}_3$ , and  $\text{MgO}$ ), as well as eight Chinese coal ash samples. The computer software package FactSage has been used to calculate the temperatures corresponding to different proportions of liquid phase of synthetic ash samples. An empirical liquidus model has been derived to correlate the  $T_{cv}$  values of the 40 synthetic ash samples with their liquidus temperatures calculated by FactSage. This model was then used to predict the  $T_{cv}$  values of the coal ash samples.

## Experimental

### Coal ash and synthetic ash samples

Eight representative Chinese coal samples were used in the study. The coal ash samples were prepared in a muffle

Correspondence concerning this article should be addressed to W. Song at zhuzb@ecust.edu.cn.

**Table 1. Ash Composition, AFTs, Liquidus Temperatures, Measured  $T_{cv}$  Values, and Critical Viscosities for Coal Ash and Synthetic Ash Samples**

Sample	Composition (wt %)					A/B <sup>a</sup>	Ash fusion temperature (°C)				$T_{cv}$ Exp (°C)	$\eta$ (Pa.s)
	SiO <sub>2</sub>	Al <sub>2</sub> O <sub>3</sub>	CaO	Fe <sub>2</sub> O <sub>3</sub>	MgO		IDT	ST	HT	FT		
Yulin	36.74	12.00	28.81	10.23	7.83	1.04	1130	1160	1185	1230	1290	38.23
Huafeng	37.16	19.92	26.65	5.75	6.04	1.48	1075	1150	1170	1185	1298	15.11
Shierkuang	42.00	20.67	12.63	15.44	2.83	2.03	1185	1210	1255	1285	1323	24.89
Wulanqiceng	45.19	19.42	13.18	17.34	0.69	2.07	1205	1235	1250	1290	1331	19.58
Huainan No.2	44.36	24.82	24.62	3.15	0.91	2.41	1285	1310	1325	1340	1424	24.35
Huainan No.1	46.66	26.10	20.63	3.31	0.96	2.92	1320	1395	1410	1420	1471	33.14
Dazhuang	49.36	24.93	12.21	9.13	1.51	3.25	1200	1210	1265	1300	1398	17.73
Gaoyang	43.11	36.67	9.48	5.25	1.94	4.79	1395	1420	1455	1475	1550	32.38
1	35.71	14.28	15.00	15.00	20.00	1.00	1155	1200	1210	1250	1413	24.98
2	31.20	20.80	30.00	15.00	3.00	1.08	1125	1170	1185	1230	1333	22.51
3	37.14	14.86	30.00	15.00	3.00	1.08	1060	1130	1150	1180	1287	25.33
4	37.86	15.14	15.00	15.00	17.00	1.13	1140	1180	1190	1225	1380	24.83
5	35.20	23.80	25.00	15.00	1.00	1.33	1080	1145	1160	1180	1310	42.58
6	40.71	16.29	15.00	25.00	3.00	1.33	1135	1185	1200	1250	1300	34.11
7	34.20	22.80	25.00	15.00	3.00	1.33	1080	1130	1165	1200	1317	13.52
8	43.57	17.43	15.00	15.00	9.00	1.56	1200	1135	1175	1210	1285	26.71
9	40.62	21.38	30.00	5.00	3.00	1.63	1100	1170	1175	1190	1307	52.50
10	44.29	17.71	15.00	20.00	3.00	1.63	1100	1155	1160	1190	1293	34.45
11	44.29	17.71	30.00	5.00	3.00	1.63	1090	1150	1160	1185	1307	31.22
12	42.59	22.41	15.00	15.00	5.00	1.86	1140	1175	1180	1210	1320	35.85
13	46.43	18.57	15.00	15.00	5.00	1.86	1100	1160	1165	1200	1314	37.34
14	36.55	30.45	15.00	15.00	3.00	2.03	1200	1250	1265	1310	1390	28.34
15	47.85	19.16	25.00	5.00	3.00	2.03	1165	1205	1220	1250	1340	18.88
16	43.90	23.10	15.00	15.00	3.00	2.03	1170	1210	1225	1280	1334	23.04
17	43.90	23.10	25.00	5.00	3.00	2.03	1180	1240	1255	1290	1389	17.25
18	46.06	20.94	15.00	15.00	3.00	2.03	1155	1200	1215	1255	1314	26.72
19	40.20	26.80	15.00	15.00	3.00	2.03	1180	1240	1255	1290	1355	16.06
20	15.46	51.54	15.00	15.00	3.00	2.18	1360	1410	1415	1455	1533	10.34
21	25.13	41.87	15.00	15.00	3.00	2.18	1350	1355	1360	1385	1500	17.11
22	43.90	23.10	15.00	15.00	3.00	2.09	1210	1250	1275	1310	1395	35.48
23	49.64	19.86	15.00	15.00	0.50	2.27	1200	1240	1250	1290	1364	30.41
24	49.50	22.50	10.00	15.00	3.00	2.57	1150	1215	1225	1275	1345	40.10
25	47.17	24.83	10.00	15.00	3.00	2.57	1180	1225	1240	1300	1346	30.08
26	43.20	28.80	15.00	10.00	3.00	2.57	1230	1285	1290	1315	1421	65.52
27	51.43	20.57	20.00	5.00	3.00	2.57	1275	1280	1300	1350	1385	45.77
28	51.43	20.57	10.00	15.00	3.00	2.57	1185	1210	1225	1245	1303	17.33
29	39.27	32.73	15.00	10.00	3.00	2.57	1270	1320	1330	1345	1433	37.16
30	51.43	20.57	15.00	10.00	3.00	2.57	1170	1215	1230	1280	1349	16.66
31	47.17	24.83	20.00	5.00	3.00	2.57	1250	1270	1285	1320	1427	40.75
32	47.17	24.83	15.00	10.00	3.00	2.57	1190	1240	1250	1285	1395	24.63
33	49.50	22.50	15.00	10.00	3.00	2.57	1175	1225	1235	1265	1367	25.20
34	52.94	24.06	5.00	15.00	3.00	3.35	1225	1265	1270	1335	1421	25.77
35	50.45	26.55	5.00	15.00	3.00	3.35	1225	1270	1290	1315	1435	21.64
36	55.00	22.00	15.00	5.00	3.00	3.35	1195	1225	1240	1325	1370	38.15
37	42.31	37.19	15.00	5.00	0.50	3.87	1330	1390	1410	1370	1455	12.35
38	57.14	22.86	2.00	15.00	3.00	4.00	1235	1280	1295	1340	1416	45.90
39	57.86	23.14	15.00	1.00	3.00	4.26	1225	1270	1280	1325	1407	23.46
40	45.27	37.73	5.00	5.00	7.00	4.88	1400	1420	1425	1440	1523	17.04

A/B=(SiO<sub>2</sub>+Al<sub>2</sub>O<sub>3</sub>)/(Fe<sub>2</sub>O<sub>3</sub>+CaO+MgO); 1-40: synthetic ash sample;  $\eta$ : Critical viscosity

furnace at 815°C for 24 h according to the Chinese standard GB/T1574-1995. Chemical analysis of the coal samples was carried out using X-ray fluorescence (XRF). Forty synthetic ash samples, covering the range of composition of most of the Chinese coal ash samples, were prepared from Sino-pharm Chemical Reagent Corp. Laboratory reagent silicon dioxide, aluminum oxide, ferric oxide, calcium oxide and magnesium oxide. The chemical composition of coal ash and synthetic ash samples is given in Table 1.

#### Ash fusion temperature test

We performed the ash fusion temperature tests by following the Chinese standard procedures (GB/T 219-1996) in a registered independent laboratory.<sup>12</sup> This test involved heat-

ing a sample cone of specified geometry at a rate of 5 K/min in an Ar atmosphere. The following specific temperatures are recorded for each sample, corresponding to specific shapes of the ash cones: Initial deformation temperature (IDT), softening temperature (ST), hemispherical temperature (HT), and flow temperature (FT). Table 1 presents the AFT data for coal ash and synthetic ash samples in an Ar atmosphere.

#### Measurement of $T_{cv}$

The apparatus for measurements of slag viscosity and  $T_{cv}$  value were described previously.<sup>13</sup> Viscosity measurements were then taken at the temperature at which the viscosity of slag was lower than 5.00 Pa·s with a bob speed of 25 rpm in

an Ar atmosphere. The higher partial pressure of oxygen was controlled by Ar/O<sub>2</sub> gas mixtures. Meanwhile, the lower partial pressure of oxygen was controlled by pure Ar gas; in addition, sacrificial graphite was used to remove few remaining oxygen in the Ar gas stream. The partial pressure of the oxygen was measured as approximately  $10^{-6}$  atm at 1200–1500°C. The viscosity measurements were taken at 20°C intervals with stirring during the stepwise cooling process, allowing for equilibration of at least 60 min after each measurement. The  $T_{cv}$  value of the coal ash sample was determined based on the definition given by Dam-Johansen et al.<sup>6</sup> Their definition indicates a point of very abrupt change in the viscosity-temperature relationship. The measured  $T_{cv}$  values and critical viscosities of studied slag are listed in Table 1.

### Thermodynamic modeling

Thermodynamic computer package FactSage<sup>14</sup> was used for predictions of multiphase equilibrium, liquidus temperatures and proportions of the liquid and solid phases in the Ar atmosphere for the multicomponent system SiO<sub>2</sub>-Al<sub>2</sub>O<sub>3</sub>-CaO-Fe<sub>2</sub>O<sub>3</sub>-MgO. All available thermodynamic and phase formation data for this system were evaluated simultaneously in order to obtain a set of model equations for the Gibbs' energy of all phases; these then corresponded to functions of temperature and composition. FactSage could automatically predict the proportion of ferric and ferrous iron oxides as a function of composition, temperature, and gas atmosphere.<sup>15</sup>

FactSage performs complex thermodynamic model calculations (quasi-chemical and sublattice) for multicomponent and multiphase systems. It uses global conditions in elementary values, temperature, and total pressure as inputs. Global conditions could also be used as target variables after defining a target and represent the interaction of components for phase formation. The most frequently used targets are the given values of an extensive property, formation or disappearance of target phase, precipitation from target phase, or equilibrium mole fraction or activity.<sup>16</sup>

In this study, we used the method of Jak et al.<sup>17</sup> where thermodynamic properties calculated for samples by FactSage have been predicted from a five-component system SiO<sub>2</sub>-Al<sub>2</sub>O<sub>3</sub>-Fe<sub>2</sub>O<sub>3</sub>-CaO-MgO, including, liquidus temperatures (temperatures at which first solid just starts to precipitate on cooling of a slag-liquid oxide melt), and the corresponding temperatures with different proportions of liquid phase. Once the phases have been determined, a total mass balance verifies the consistency of the system. For example, a four-component system of SiO<sub>2</sub>-Al<sub>2</sub>O<sub>3</sub>-FeO-CaO (63.1, 27.7, 6.10 and 3.10 wt %, respectively), with the addition of  $10 \pm 1.5$  g FeO per 100 g of initial sample, was selected for subsequent calculations.<sup>18</sup> As temperature decreased below the liquidus, the proportion of the mullite phase (3Al<sub>2</sub>O<sub>3</sub>·2SiO<sub>2</sub>) increased and the liquid proportion of the liquid phase decreased. At a temperature of approximately 1380°C, the tridymite phase (SiO<sub>2</sub>) started to precipitate (in addition to the mullite phase). At approximately 1150°C, anorthite (CaO·Al<sub>2</sub>O<sub>3</sub>·2SiO<sub>2</sub>) started to form. Meanwhile, the mass of liquid and solid phases remained conservative from the single phase, to multiphase, and to liquid phase. For

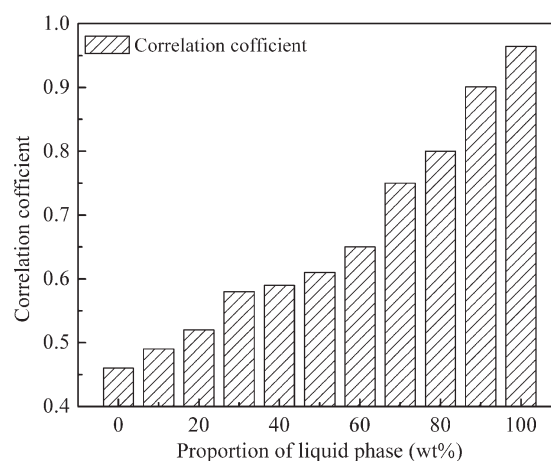


**Figure 1. The effect of proportion of liquid phase on the correlation coefficients between the measured  $T_{cv}$  values and temperatures corresponding to different proportions of liquid phase for synthetic ash samples.**

instance, at above 1550°C, the system comprised 100 g liquid phase; at 1300°C, the system comprised 71 g of liquid phase, 14 g of solid tridymite, and 15 g of solid mullite phase.

## Results and Discussion

### Development of the $T_{cv}$ correlation

Linear regression analysis was used to compare the correlations between the  $T_{cv}$  values of synthetic ash samples and the corresponding temperatures with different proportions of liquid phase calculated by FactSage. Generally, the reliability of the values calculated using such correlations is indicated by the correlation coefficient (R). The standard deviation,  $\sigma$  value, simply indicates how close the calculated value is to the experimental values. In our work, the R values have been used to analyze the correlations between the  $T_{cv}$  values of synthetic ash samples and their temperatures with different proportions of liquid. An R value of 0.7 is generally acceptable for predicting the  $T_{cv}$  values of ash samples, a value of 0.8 is good and 0.9 or higher is excellent.<sup>7</sup>

Figure 1 presents the effect of proportion of liquid phase on the correlation coefficients between the  $T_{cv}$  and the corresponding temperatures with different proportions of liquid phase calculated by FactSage for synthetic ash samples. Observations from Figure 1 indicate an increase in the  $T_{cv}$  corresponding to R values corresponding to the  $T_{cv}$  of synthetic ash samples as the proportion of liquid calculated by FactSage increases. When the proportion of liquid exceeds 70%, the value of the correlation coefficient is higher than 0.7. In particular, when the proportion of liquid increases to 100%, the corresponding R value for the  $T_{cv}$  is higher than 0.9, which is indicative of a significant correlation between the  $T_{cv}$  values of the synthetic ash samples and the liquidus temperature calculated by FactSage.

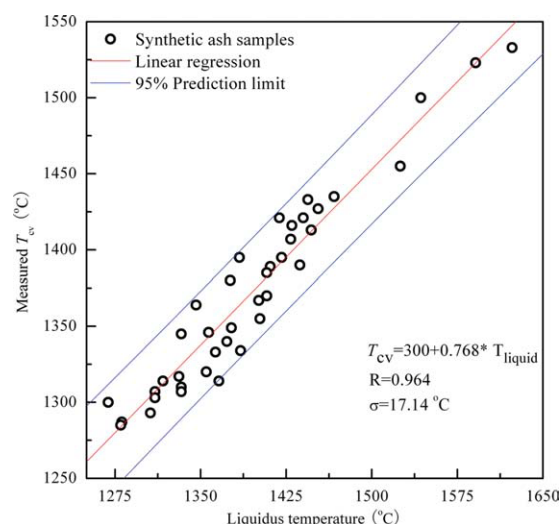


**Figure 2. Correlation between the measured  $T_{cv}$  values and liquidus temperatures of synthetic ash samples.**

[Color figure can be viewed in the online issue, which is available at [wileyonlinelibrary.com](http://wileyonlinelibrary.com).]

Figure 2 shows the  $T_{cv}$  of the synthetic ash samples as a function of the calculated liquidus temperatures. Good correlations between the  $T_{cv}$  and liquidus temperatures can clearly be seen: the higher the liquidus temperature—the higher the  $T_{cv}$ . Moreover, the  $\sigma$  value is less than  $20^{\circ}\text{C}$ , which indicates that the accuracy of the results is within the experimental error.

The  $T_{cv}$  of the synthetic ash samples could be expressed as a linear function of the liquidus temperature according to the equation

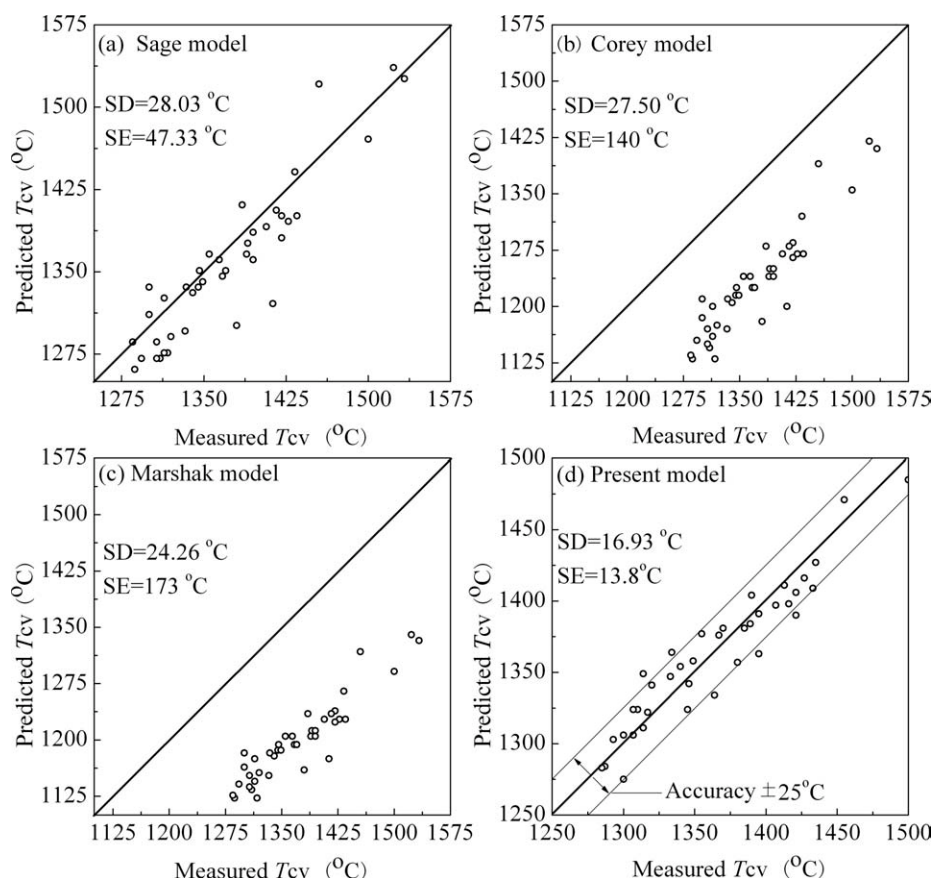
$$T_{CV} = 300 + 0.768 \cdot T_{Liquidus} \quad (4)$$

where  $T_{liquidus}$  is the liquidus temperature of the sample in degrees celsius ( $^{\circ}\text{C}$ ).

### Comparison of the models

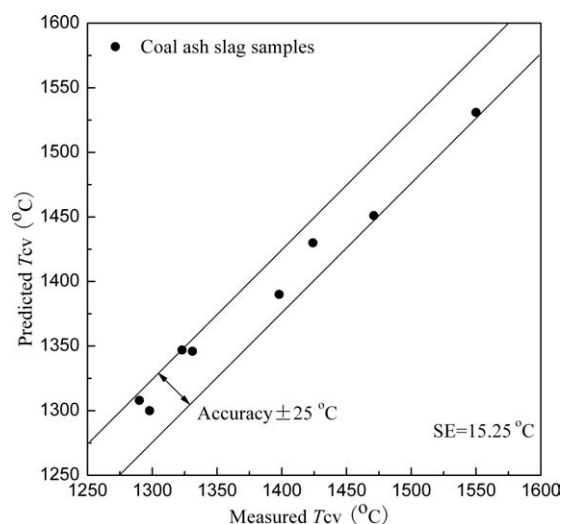
To test the accuracy of the various methods, the experimental  $T_{cv}$  values of the synthetic ash samples were compared to predictions by each of models mentioned in the Introduction.

Figure 3 shows parity plots of the measured  $T_{cv}$  values vs. those predicted for synthetic ash samples by the Sage model,



**Figure 3. Comparison of the measured  $T_{cv}$  values with those predicted by (a) the Sage model, (b) the Corey model, (c) the Marshak model, and (d) the liquidus model for synthetic ash samples.**





**Figure 4. Comparison between measured and predicted  $T_{cv}$  values for coal ash samples.**

the Corey model, the Marshak model, and the liquidus model, respectively. As can be seen from Figure 3a–c, these correlations significantly differ from the experimental measurements. Figure 3d shows a parity plot of measured  $T_{cv}$  values vs. those predicted for the synthetic ash samples by the liquidus model (Eq. 4). This model has the lowest bias and standard error, which is also demonstrated by the data lying close to the equivalence line. Most of the synthetic ash samples show deformation temperatures within experimental errors of  $\pm 25^\circ\text{C}$ ; therefore, this model (Eq. 4) can predict  $T_{cv}$  of synthetic ash samples in an Ar atmosphere.

#### Prediction $T_{cv}$ of Coal Ash Samples

In our work, the liquidus model (Eq. 4) was used to predict the  $T_{cv}$  of coal ash samples. Figure 4 shows a parity plot of the measured  $T_{cv}$  vs. the predicted  $T_{cv}$  for the eight Chinese coal ash samples. It can be seen that all of the coal ash samples show deformation temperatures within experimental errors of  $\pm 25^\circ\text{C}$ , which indicates that the liquidus model can predict  $T_{cv}$  of coal ash samples with a good level of accuracy.

#### Conclusion

In our work, an empirical equation has been derived to relate the  $T_{cv}$  of 40 synthetic ash samples with their liquidus temperature calculated by FactSage. An apparent linear correlation and good agreement between the  $T_{cv}$  of synthetic ash samples and the liquidus temperatures calculated by FactSage ( $R > 0.90$ ,  $\sigma < 20^\circ\text{C}$ ) has been found. This equation has been used to predict the  $T_{cv}$  of eight Chinese coal ash samples with a good level of accuracy ( $SE < 20^\circ\text{C}$ ).

#### Acknowledgments

We would like to thank Prof. Xuedong Zhu, Prof. Lihua Tang, Prof. Qi Zhang of East China University of Science and Technology for their valuable discussions and for sustained encouragement. We would also like to thank Prof. Zhanmin CaO of University of Science and Technology Beijing, research scientist Dr. Qiang Qu of GE Global Research, Ms Yi Gao, and Ms Danfeng Wang for their assistance in the application of FactSage and for validating the calculated data presented in this article. We would also like to express our gratitude to the two anonymous reviewers for their constructive comments that greatly improved the manuscript, as well as to the journal editor, Prof. Stanley I. Sandler, and to the editorial assistant, Sandra Patterson, for their great support of the manuscript.

#### Literature Cited

- Frandsen F, Dam-Johansen K, Rasmussen P. Trace elements from combustion and gasification of coal-an equilibrium approach. *Progr Energy Combust Sci.* 1994;20:115–138.
- Hurst HJ, Novak F, Patterson JH. Viscosity measurements and empirical predictions for fluxed Australian bituminous coal ashes. *Fuel.* 1999;78:1831–1840.
- Higman C, Van Der Burgt M. *Gasification*. 2nd ed. Boston: Elsevier/Gulf Professional Publishing Publications; 2008.
- Song W, Tang L, Zhu X, Wu Y, Rong Y, Zhu Z, Koyama S. Flow properties and rheology of slag from coal gasification. *Fuel.* 2010; 89:1709–1715.
- Browning GJ, Bryant GW, Hurst HJ, Lucas JA, Wall TF. An empirical method for the prediction of coal ash slag viscosity. *Energy Fuels.* 2003;17:731–737.
- Vargas S, Frandsen FJ, Dam-Johansen K. Rheological properties of high-temperature melts of coal ashes and other silicates. *Progr Energy Combust Sci.* 2001;27:237–429.
- Seggiani M, Pannocchia G. Prediction of coal ash thermal properties using partial least-squares regression. *Ind Eng Chem Res.* 2003;42: 4919–4926.
- Sage WL, McIlroy JB. Relationship of coal ash viscosity to chemical composition. *Combustion.* 1959;31:41–48.
- Corey RC. *Measurement and significance of the flow properties of coal-ash slag*. Washington, D.C: US Dept of the Interior, Bureau of Mines, Report No. 618; 1964:67.
- Marshak, Ryzhakov. *Determination of coal-ash properties*. In: Singer JG. *Combustion-Fossil Power*. Norwalk, CT: Combustion Engineering, Inc; 1991:1123.
- Kondratiev A, Jak E. Predicting coal ash slag flow characteristics. *Fuel.* 2001;80:1989–2000.
- Song WJ, Tang LH, Zhu XD, Wu YQ, Zhu ZB, Koyama S. Prediction of Chinese coal ash fusion temperatures in Ar and  $\text{H}_2$  atmospheres. *Energy Fuels.* 2009;23:1990–1997.
- Song W, Tang L, Zhu X, Wu Y, Rong Y, Zhu Z, Koyama S. Fusibility and flow properties of coal ash and slag. *Fuel.* 2009;88:297–304.
- Bale CW, Chartrand P, Degterov SA, Eriksson G, Hack K, Mahfoud RB, Melancon J, Pelton AD, Petersen S. FactSage thermochemical software and databases. *Calphad.* 2002;26:189–228.
- Jak E. Prediction of coal ash fusion temperatures with the F\*A\*C\*T thermodynamic computer package. *Fuel.* 2002;81:1655–1668.
- Eriksson G, Konigsberger E. FactSage and ChemApp: Two tools for the prediction of multiphase chemical equilibria in solutions. *Pure Appl Chem.* 2008;80:1293–1302.
- Kondratiev A, Jak E. Review of experimental data and modeling of the viscosities of fully liquid slags in the  $\text{Al}_2\text{O}_3\text{-CaO-FeO-SiO}_2$  system. *Metall Mater Trans B.* 2001;32B:1015–1025.
- Jak E, Degterov S, Hayes PC, Pelton AD. Thermodynamic modeling of the system  $\text{Al}_2\text{O}_3\text{-SiO}_2\text{-CaO-FeO-Fe}_2\text{O}_3$  to predict the flux requirements for coal ash slags. *Fuel.* 1998;77:77–84.

Manuscript received Aug. 26, 2010, and revision received Oct. 31, 2010.